nature geoscience

SUPPLEMENTARY INFORMATION

https://doi.org/10.1038/s41561-019-0368-9

In the format provided by the authors and unedited.

Highly heterogeneous depleted mantle recorded in the lower oceanic crust

Sarah Lambart[1,2*], Janne M. Koornneef[3], Marc-Alban Millet[1], Gareth R. Davies[3], Matthew Cook[1] and C. Johan Lissenberg[1]

[1]Cardiff University, School of Earth and Ocean Sciences, Cardiff, UK. [2]University of Utah, Department of Geology and Geophysics, Salt Lake City, USA. [3]Vrije Universiteit, Faculty of Science, Amsterdam, The Netherlands. *e-mail: sarah.lambart@utah.edu

Supplementary Figures and Table to accompany 'Highly Heterogeneous Depleted Mantle Recorded in the Lower Oceanic Crust' by Lambart et al.

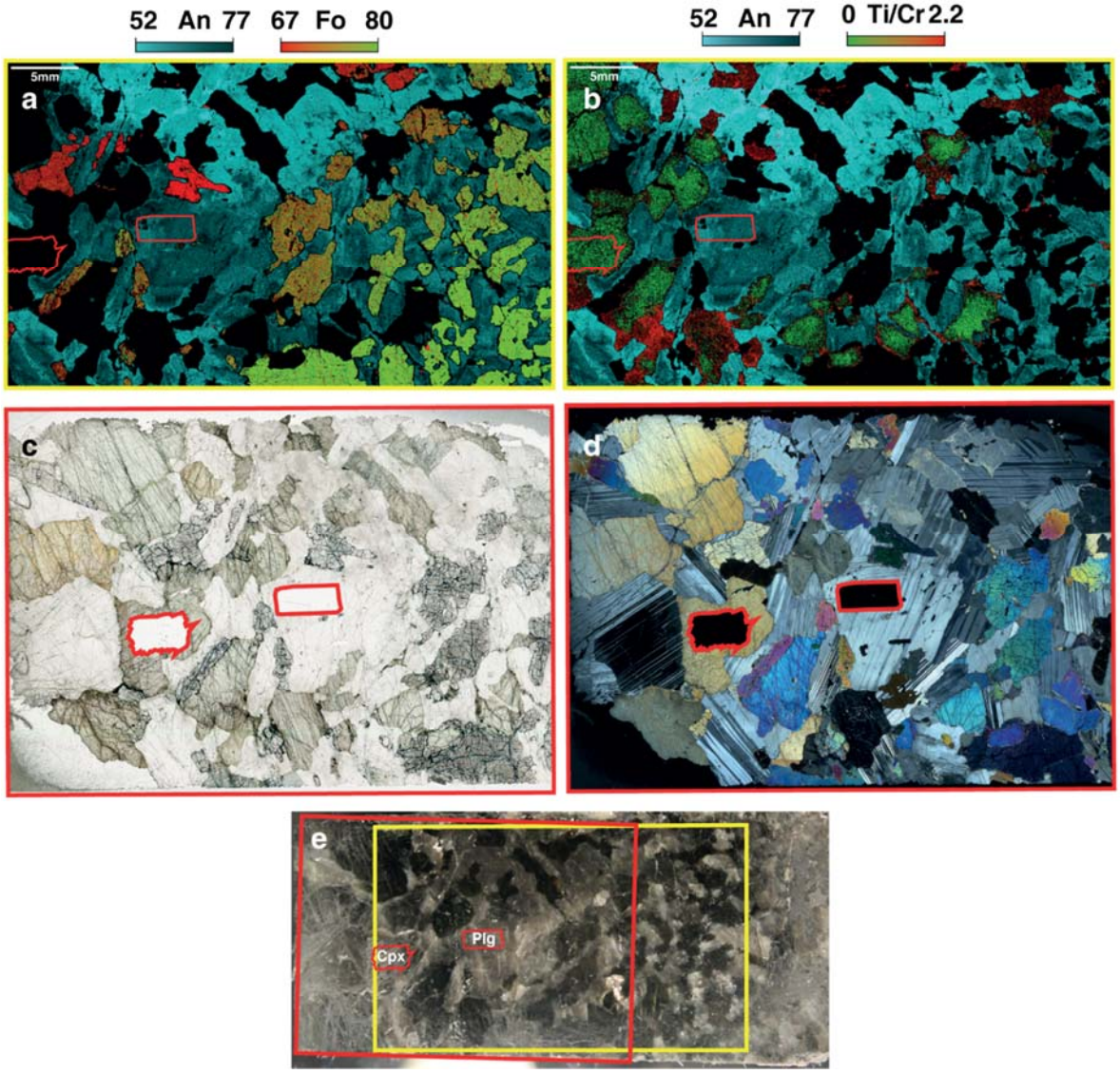

Supplementary Figure 1. Illustration of the method for selecting micro-milling sites. Mg–Fe–Na **(a)** and Ti-Cr-Na **(b)** element maps, photomicrographs **(c-d)** showing the microdrill locations, and core photo **(e)** showing the element map area (yellow), the thin section area (red) of the olivine gabbro 268R3-6-12 from IODP Hole U1309D. Map (a) shows Fo (red to green) and An (light to dark blue) content variations of olivine and plagioclase at the scale of the sample. Clinopyroxene appears black because Fe and Mg have been scaled to show the olivine compositions. Map (b) highlight An content of plagioclase and TiO_2/Cr_2O_3 ratio in clinopyroxene. Red highlighted area indicate microdrill location. A noteworthy feature is the substantial An, Fo and TiO_2/Cr_2O_3 variations on a cm scale (a-b).

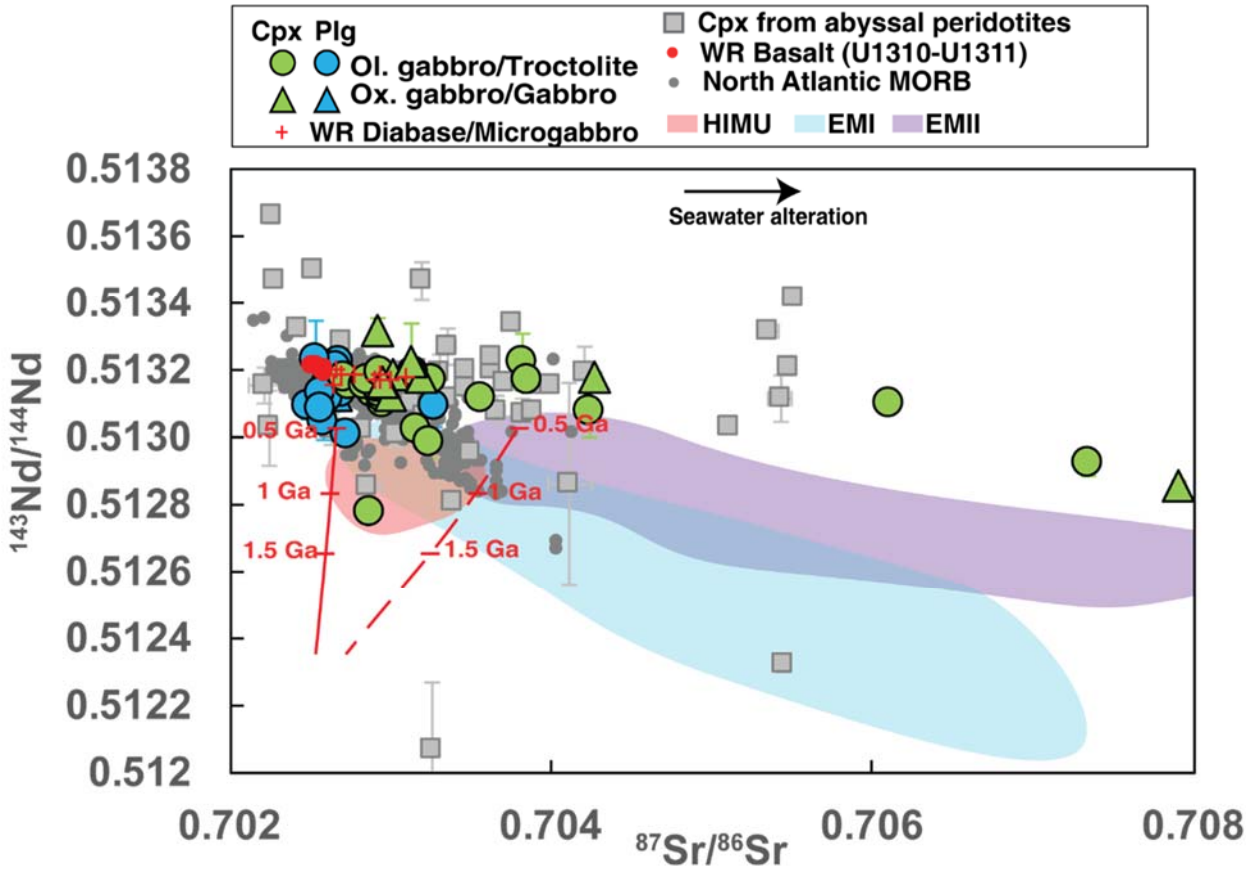

Supplementary Figure 2. Comparison between isotopic compositions analysed in this study and compositions of North Atlantic MORB. $^{143}Nd/^{144}Nd$ versus $^{87}Sr/^{86}Sr$ ratios of Atlantis Massif clinopyroxene and plagioclase compared with whole rock (WR) diabase and basalt isotopic analyses performed in this study, theNorth Atlantic MORB compositions reported in the literature (PetDB database[42]) and the clinopyroxene compositions from abyssal peridotites collected along the MAR[7,12,13]. Compositional fields of HIMU (red), EMI (blue) and EMII (purple) basalts are shown for comparison[50]. The red lines are calculated present-day isotopic compositions of recycled oceanic gabbro affected (dashed line) or not (solid line) by seawater alteration, as a function of recycling age[50]. Error bars: 2SE.

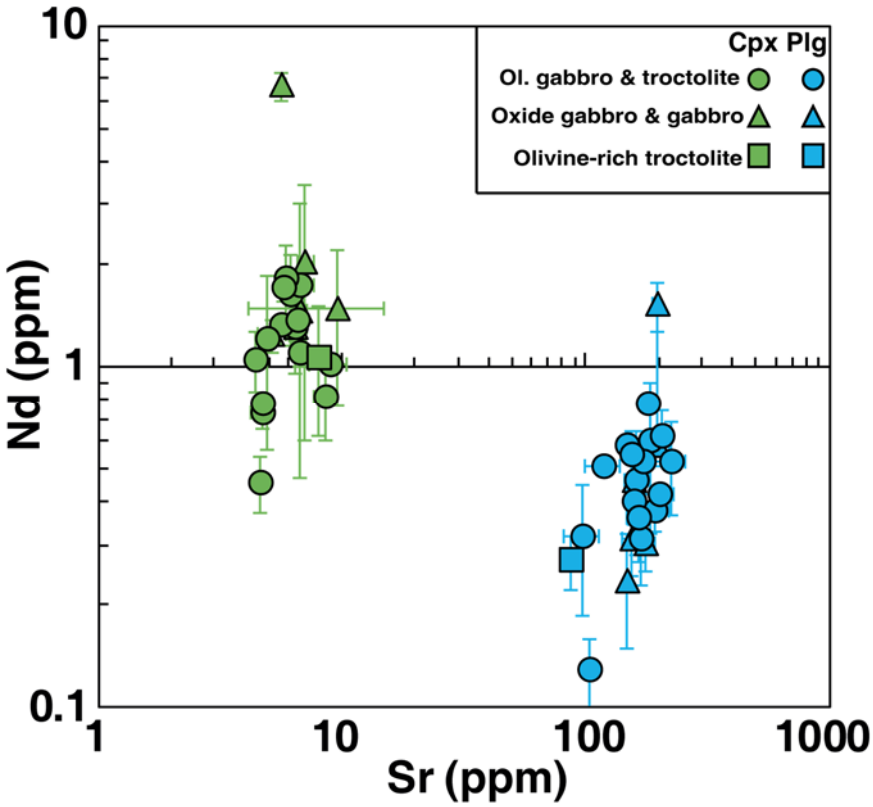

Supplementary Figure 3. Sr and Nd concentrations in selected minerals for micromilling (2σ error bars).

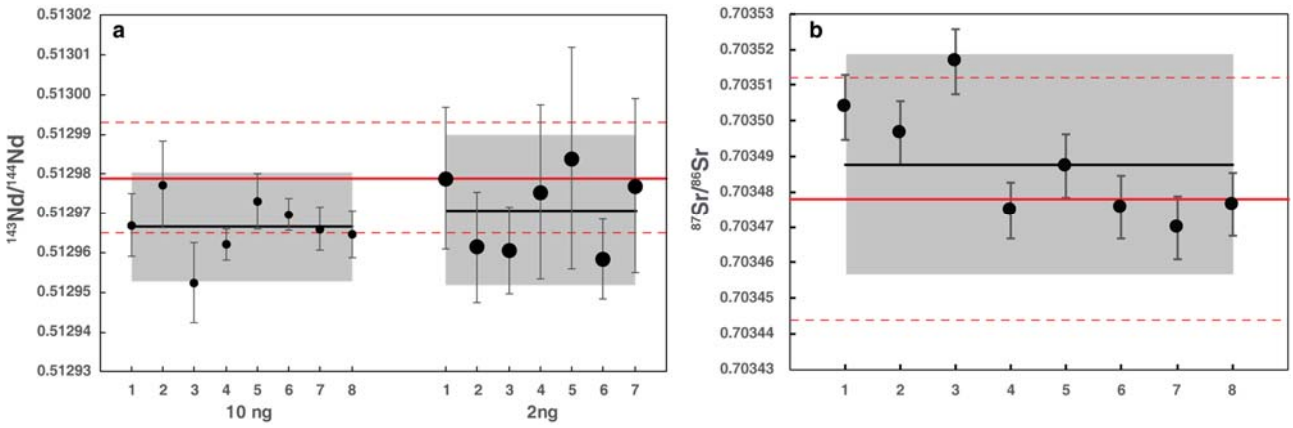

Supplementary Figure 4. Standard analyses on TIMS. a. $^{143}Nd/^{144}Nd$ ratios (2SE error bars) measured on BHVO-2. Filaments were loaded with 10 ng (small circles) or 2 ng of Nd (large circles). **b.** $^{87}Sr/^{86}Sr$ ratios (2SE error bars) measured on 200ng Sr separated from BHVO-2. Black line and grey band are the average and 2SD measured on BHVO-2 in this study. Solid and dashed red lines are average and 2SD reported for BHVO-2 in GeoReM database.

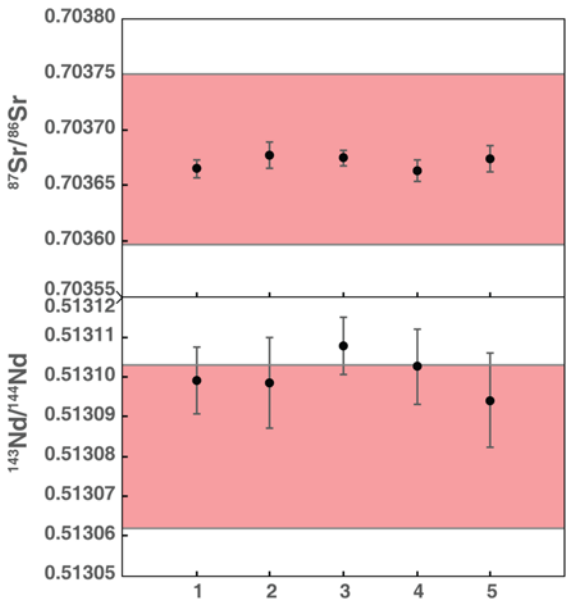

Supplementary Figure 5. Standard analyses on Nu Instrument. $^{87}Sr/^{86}Sr$ and $^{143}Nd/^{144}Nd$ ratios measured on JB-2 after correction for fractionation and mass bias (2SE error bars). Red bands are the range of values reported for JB-2 in GeoReM database.

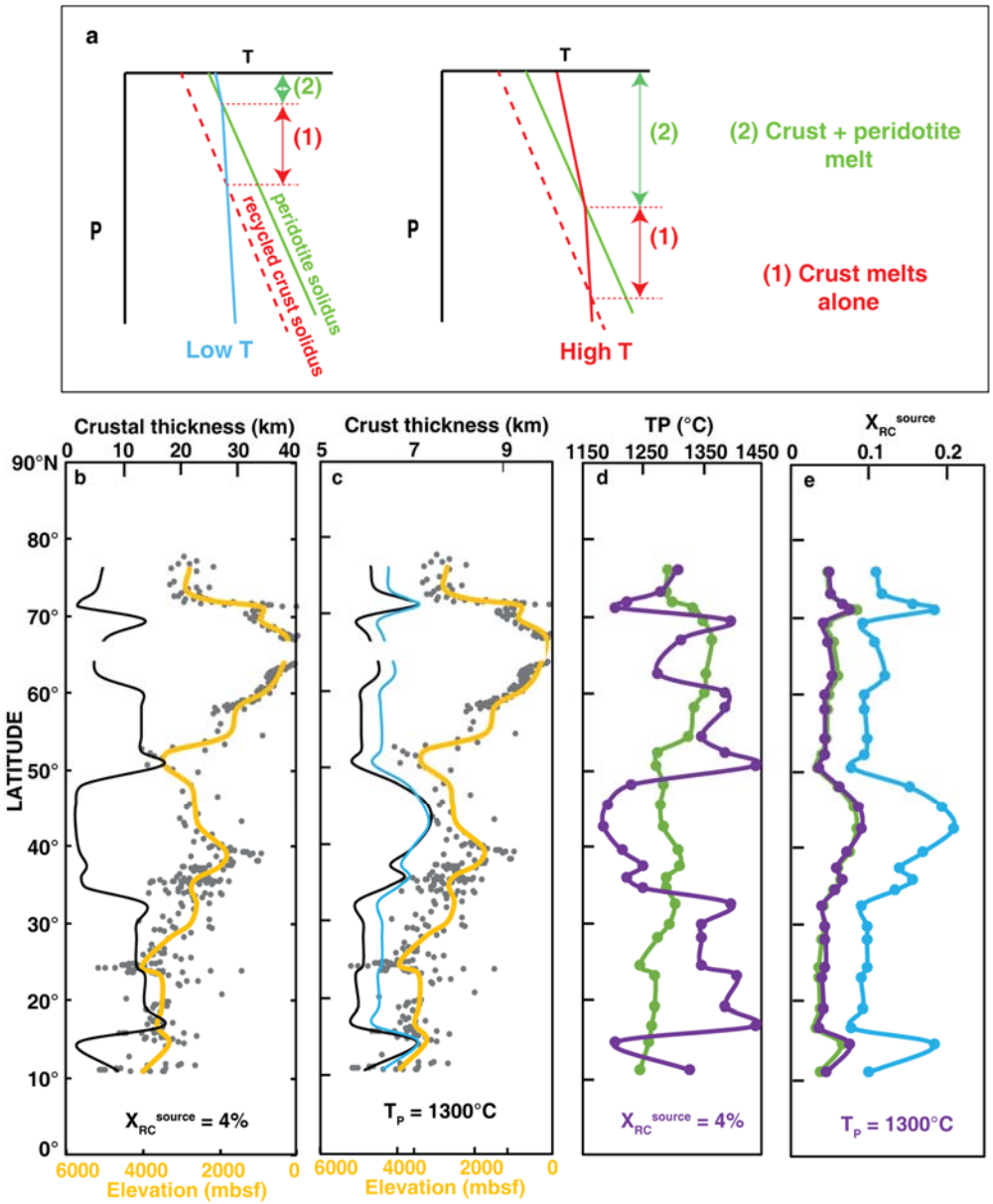

Supplementary Figure 6. Results of geochemical modelling. a. Schematic illustration of the effect of mantle potential temperature (T_P) on the fraction of recycled crust in the melt: increasing T_P decreases the ratio between the interval where only the recycled crust is melting and the interval where both crust and peridotite are melting (i.e., (1)/(2) ratio). **b-c**. Comparison between the average MORB elevations (orange line) with the calculated crust thicknesses (black line), assuming a constant fraction of recycled crust, X_{RC} = 4%, and varying T_P (b), or assuming a constant T_P = 1300°C and varying the proportion of recycled crust (c). **d.** Calculated T_P with constant X_{RC} = 4% (purple) and the hybrid model (green). **e.** Calculated X_{RC}^{source} with constant T_P = 1300°C (purple) and with the hybrid model (green). In (c) and (e), the blue line shows the results using T_P = 1300°C and the composition KG1 for the enriched material.

Supplementary Table 1. Isotopic analyses of clinopyroxenes, plagioclase and whole rocks plotted in Figs. 1&2.

Sample	depth	Plagioclase						Clinopyroxene						Whole rock	
	(mbsf)	$^{87}Sr/^{86}Sr$	Sr*	*n*	$^{143}Nd/^{144}Nd$	Nd*	*n*	$^{87}Sr/^{86}Sr$	Sr*	*n*	$^{143}Nd/^{144}Nd$	Nd*	*n*	$^{87}Sr/^{86}Sr$	$^{143}Nd/^{144}Nd$
15R1-43-45	84.54													0.703096 (9)	0.513184 (8)
36R1-48-53	196.09	0.702643 (8)	200	185	0.513169 (30)	8	114	0.703023 (10)	35	208	0.513191 (9)	30	168		
41R2-27-31a	221.25	0.702693 (8)	200	200	0.513136 (20)	2	96	0.703158 (14)	50	212	0.513024 (16)	4	181		
41R2-27-31b	221.50	0.704276 (44)	200	95				0.703823 (36)	50	54	0.513226 (87)	5	54		
54R3-125-126	285.15													0.702825 (10)	
65R1-141-143	335.42													0.702905 (11)	0.513169 (11)
73R2-124-129	375.12	0.702675 (9)	150	200	0.513224 (45)	3	59								
88R4-110-113	443.07				0.513170 (40)	1	66	0.702941 (9)	15	259	0.513135 (16)	3	82		
90R3-22-27	451.85	0.702600 (8)	200	200	0.513175 (24)	2	93	0.703196 (36)	120	501	0.513179 (3)	30	203		
104R3-113-115	519.76	0.702660 (9)	200	200	0.513127 (46)	2	77	0.703000 (8)	30	240	0.513125 (12)	8	80		
117R3-86-87	581.70													0.702999 (8)	0.513170 (8)
125R2-119-121	614.06													0.702941 (9)	0.513171 (10)
149R2-16-21	733.49	0.702611 (26)	200	200	0.513213 (40)	5	95	0.702861 (13)	30	208	0.513180 (72)	15	125		
149R2-68-71a	734.00	0.703272 (10)	200	200	0.513096 (64)	2	55	0.703238 (10)	15	222	0.512986^{+} (41)	2	94		
149R2-68-71b	734.00							0.704235 (57)	27	110	0.513078 (77)	5	56		
153R1-25-24	751.25													0.702938 (8)	0.513186 (8)
175R2-25-28	853.00	0.702662 (25)	200	100	0.513214 (34)	1	132	0.703571 (14)	50	272	0.513121 (18)	5	98		
179R4-118-123	875.33													0.702644 (7)	0.513154 (9)
187R3-23-27	911.63	0.702611 (8)	200	200	0.513121 (34)	6	74	0.702893 (9)	40	224	0.513135 (23)	10	80		
205R4-63-66	990.38													0.702698 (8)	0.513190 (9)
214R1-138-143	1031.01							0.702961 (10)	25	201	0.513106 (10)	5	139		
227R1-112-117	1093.15	0.702575 (8)	250	200	0.513179 (36)	2	76	0.702963 (10)	25	219	0.513163 (23)	5	86		
227R2-28-33	1093.74	0.702732 (8)	200	189	0.513012 (33)	3	108	0.702959 (10)	35	203	0.513116 (10)	5	135		
229R1-66-71	1102.29	0.702566 (8)	200	180	0.513090 (30)	3	131	0.702744 (8)	40	200	0.513155 (10)	10	93		
242R2-35-39	1174.37	0.702488 (9)	200	240	0.513099 (44)	2	79	0.702941 (10)	50	333	0.513137 (12)	17	81		
249R1-54-56	1197.25	0.702564 (9)	200	200	0.513134 (30)	3	83	0.702719 (10)	60	200	0.513177 (16)	12	58		
250R1-83-87	1202.35				0.513019 (184)	1	40	0.702836 (9)	30	301	0.513157 (20)	7			
250R2-60-66	1203.59	0.702530 (9)	200	200	0.513236 (116)	3	84				0.513235 (22)	20	121		
251R1-60-65	1206.93	0.702569 (9)	150	181				0.703256 (60)	10	88	0.513172 (17)	4	136		
251R3-59-62	1209.77							0.704269 (18)	15	241	0.513179 (16)	5	136		
252R4-3-6a	1215.43	0.702612 (6)	170	340	0.513174 (33)	2	106	0.702920 (9)	30	208	0.513207^{+} (23)	5	84		
252R4-3-6b	1215.43	0.702633 (8)	200	192				0.703130 (16)	80	155	0.513230 (109)	16	45		
252R4-3-6c	1215.43							0.707908 (11)	49	134	0.512857 (18)	10	67		
253R1-40-41	1216.31													0.702618 (8)	0.513204 (9)
253R3-0-3	1218.63													0.702600 (10)	
253R3-45-78	1219.07							0.702927 (8)	15	222	0.513151 (15)	2	97		
257R1-95-100a	1236.08	0.702594 (9)	200	200	0.513048 (56)	3	64	0.702884 (9)	30	240	0.512800^{+} (15)	5	73		
257R1-95-100b	1236.08	0.702574 (15)	200	119	0.513088 (49)	6	75	0.707341 (11)	41	103	0.512927 (38)	11	68		
257R1-95-100c	1236.08							0.706109 (12)	82	193	0.513100 (16)	22	65		
257R1-95-100d	1236.08							0.703154 (50)	44	63	0.513192 (26)	12	55		

Table S1. *Continued*

Sample	depth	Plagioclase						Clinopyroxene						Whole rock	
	(mbsf)	$^{87}Sr/^{86}Sr$	Sr*	*n*	$^{143}Nd/^{144}Nd$	Nd*	*n*	$^{87}Sr/^{86}Sr$	Sr*	*n*	$^{143}Nd/^{144}Nd$	Nd*	*n*	$^{87}Sr/^{86}Sr$	$^{143}Nd/^{144}Nd$
260R1-14-16	1249.65													0.702664 (7)	0.513205 (7)
268R2-78-81	1290.03	0.702574 (8)	300	200				0.702865 (12)	35	227	0.513175 (17)	10	100		
268R3-6-12	1290.69				0.513301 (104)	2	73	0.702937 (9)	30	380	0.513194 (12)	10	108		
287R1-6-8	1377.67													0.702779 (8)	0.513191 (9)
292R1-75-77	1397.56				0.513169 (136)	1	80	0.703858 (14)	40	227	0.513168 (30)	9	39		
1310-A1-0-13	0.07													0.702576 (9)	0.513214 (11)
1310-A1-13-19	0.16													0.702567 (10)	0.513210 (11)
1310-B1R1-0-5	0.03													0.702572 (8)	0.513203 (10)
1310-B1R1-62-69	0.66													0.702560 (9)	0.513207 (16)
1310-B1R1-139-143	1.41													0.702572 (9)	0.513198 (9)
1311-AR1-0-9	0.05													0.702515 (10)	0.513220 (11)
1311-AR1-48-54	0.51													0.702528 (8)	0.513223 (9)
1311-AR1-99-104	1.02													0.702525 (9)	0.513225 (11)
1311-AR1-136-142	1.39													0.702499 (5)	0.513226 (9)

2 SE (in parentheses) are given in terms of least unit cited: e.g., 0.702643 (8) represent 0.70264 ± 0.000008.

n: number of cycles for each analyses

* Amount of Sr and Nd (in ng) analysed calculated from Sr and Nd concentration and estimated volume of milled mineral

+ $^{143}Nd/^{144}Nd$ ratios uncorrected for Sm: 0.512936±31 for 149R2-68-71a, 0.513169±19 for 252-R4-3-6a and 0.512783±15 for 257R1-95-100a.